Proceedings World Geothermal Congress 2005
Antalya, Turkey, 24-29 April 2005

Controlled Source Magnetotelluric (CSMT) Survey of Malabuyoc Thermal Prospect, Malabuyoc/Alegria, Cebu, Philippines

R.A.Del Rosario, Jr., M.S. Pastor and R.T. Malapitan

Geothermal and Coal Division, Energy Resource Development Bureau, Department of Energy, Energy Center, Merritt Road, Ft. Bonifacio, Taguig, MM, Philippines

rogelio_delrosario65@yahoo.com, mikepastor68@yahoo.com, ruelmalapitan@yahoo.com

Keywords: Controlled Source Magnetotelluric, Malabuyoc, MRF

ABSTRACT

The Controlled Source Magnetotelluric (CSMT) survey conducted at Malabuyoc geothermal prospect aims at establishing the presence and extent of hot water to a medium depth of 300-500 meters for non-electrical applications of geothermal fluids.

The resistivity anomalies in the prospect are largely controlled by geologic structure (faulted anticlinal structure).

The Malabuyoc system is categorized as a basement aquifer beneath a sedimentary basin with the heated fluid probably originating at the center of the basin east of the survey area. The fluid is channeled along the Middle Diagonal and Montañeza River Faults (MRF) and emerged along the stretch of Montaneza River as warm seepages.

The best site to drill for a well that could extract possible hot/warm water for spa resort development is the area bounded by steep resistivity gradient coincident with MRF. Possible hot water is at permeable karst aquifer located at depth between the –100 to –300 m below sea level (bsl).

1. INTRODUCTION

The Controlled Source Magnetotelluric (CSMT) survey was conducted over the Malabuyoc Geothermal Prospect from May 16, 2002 - June 8, 2002 covering the towns of Malabuyoc and a portion of Alegria, in Cebu Province. The survey is the Department of Energy's (DOE's) commitment in the Health Spa Resort Development Project, an inter-agency collaboration between the Department of Tourism (DOT), Department of Energy (DOE) and Philippine Institute of Traditional and Alternative Health Care-Department of Health (PITAHC-DOH). The project objective is to promote identified geothermal areas for health spa resort development while the survey is to establish the presence and extent of hot water at a medium depth between 300-500 meters for non-electrical applications. This technique has been used successfully in the exploration of shallow groundwater resources in the United States (Zonge, 1992).

1.1 Location and Accessibility

The Malabuyoc Geothermal Prospect Area (MGPA) is located in Cebu Island (Figure 1). Cebu Island is situated between the islands of Negros in the west, Bohol and Leyte on the east, Siquijor on the south and Masbate on the north. Cebu City is the capital of the province located midway on the eastern coast of the island. It is accessible by air, land and sea.

From Cebu City, the town of Malabuyoc is about 123 kms or 4-hour drive via Car-Car-Dalaguete-Ginatilan Provincial Highway or about 3-hour via Car-Car Barili Road going south to Ginatilan. From Malabuyoc proper, the thermal spring is located north-northwest in Brgy. Montaneza. It could be reached via barangay road leading to Sitio Mainit, where the thermal spring is situated.

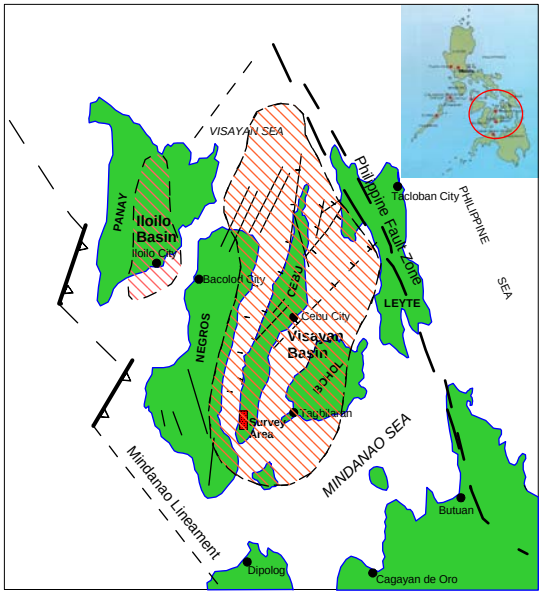

Figure 1: Tectonic Scenario of Cebu Province

1.2 Regional Geologic and Tectonic Setting

The whole island of Cebu, together with parts of Negros and Bohol Islands, lies within the Visayan Basin, a N-S trending structural basin consisting of horst and graben and several small-interconnected sub-basins (BED, 1985) (Fig. 1). It is bounded on the east by the Philippine Fault and on the west by the probable extension of Mindanao Lineament. Cebu Island is situated near the center of the Visayan Basin forming a structural high separated from Negros and Bohol by downfaulted blocks. Structural trends are generally northwesterly in the southern part and northerly in the northern part.

Forming the backbone of Southern Cebu is the Late Cretaceous to Paleocene Pandan Formation consisting of metamorphosed limestone, shale and conglomerate with lenses of lava flows and coal (Barnes, 1956; Hashimoto and Balce, 1977; Alcantara, 1980; BMG, 1981) (Fig. 2). Intruding Pandan Formation were several fine to medium grained andesite sills and dykes (Barnes, 1956). The intrusions are generally concordant with Pandan but in places cut through the sedimentary rocks as dykes. Pandan Formation is unconformably overlain by the Argao Group

(Barnes, 1956) of Late Oligocene to Early Miocene age consisting of three members: Calagasan Formation, Bugtong Limestone and Linut-Od Formation. Alcantara (1980) added a fourth member, the Mantalongon limestone. Calagasan Formation is composed of conglomerate, sandstone and shale with limestone and coal interbeds while Bugtong Limestone is massive to thin bedded, white to light brown and yellowish gray, fine to medium grained relatively dense crystalline to shaly and sandy limestone deposited in shallow warm seas during Early Miocene. The two are overlain by the Linut-Od Formation consisting of Lower Miocene coal-bearing sequence of clastic rocks similar in lithology to Calagasan. In turn, the Linu-Od is overlain by Mantalongon Limestone, a Miogypsina and lepidocyclina bearing limestone blocks in Argao-Dalaguete region. Argao Group is equivalent to Naga Group of Santos-Ynigo and Cebu and Malubog Formations of Corby (1951) and BED (1985) in Central and Northern Cebu. Widespread in the area is the Barili Formation (MGB, 1981) of Late Miocene to Pliocene consisting of lower limestone member and upper marl member. The limestone is light brown, hard, corraline, locally porous or sandy, richly fossiliferous while the marl is poorly bedded, generally brown, slightly sandy, fossilferous with thin limestone interbed. Together with Mt. Uling Limestone, Toledo and Carcar Formation, Barili formation was initially included in the Balamban group of Barnes (1956) and Santos-Ynigo (1967). Occupying the lower flanks of the ridges and covering almost all of the coastal areas is the Pleistocene Carcar Formation. It is a shallow marine, porous, coralline, massive to poorly bedded limestone deposit that is rich in mollusk, coral stems, algae and foraminifera.

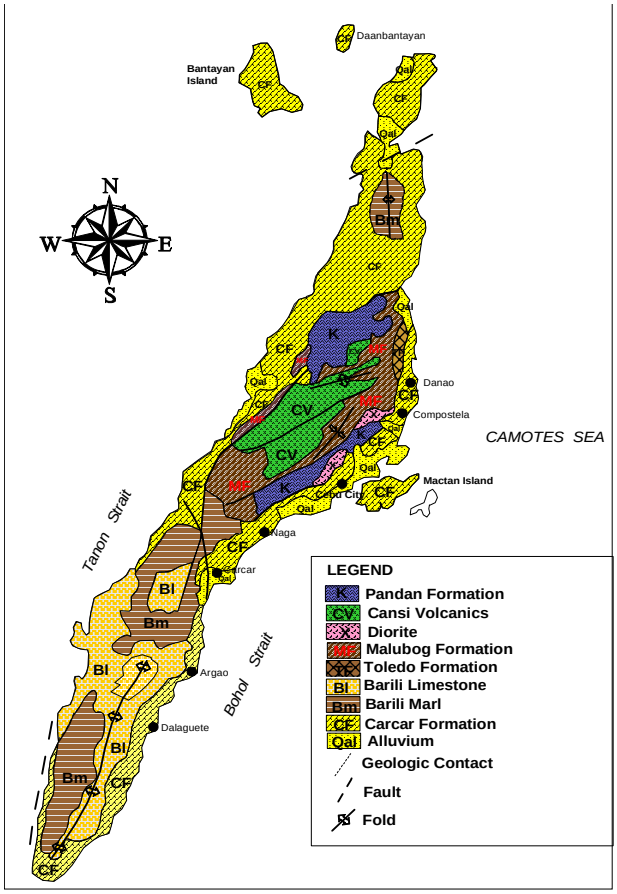

Figure 2: General Geology of Cebu Province

1.3 Local Geology and Structures

The survey area is located along the western flank of an 18-kilometer long and 3 kilometer wide NNE trending plunging asymmetrical anticline. (CPRS, 1974 and BED-ELC, 1979) (Fig. 3). This anticline is separated into two by the NW-SE trending strike slip fault at the vicinity of Legaspi River namely: the Alegria structure in the north and the Malabuyoc structure in the south. On the surface the Malabuyoc Anticline a length of 6 kilometer and a width of 3 kilometer trends NNE. A diagonal fault runs across the middle part of this anticline with the northern block forming an upthrown structure favorable for trapping hydrocarbon (CPRS, 1976). The northern block was offset left-laterally by another WNW trending fault called by the present study as the Montañeza River Fault (MRF) (BED-ELC, 1979). MRF pass through the Montañeza River and was manifested in the field by abrupt topographic break and alignment of thermal spring along the Montañeza River (Malapitan and Del Rosario, 2002). South of the thermal area, a North-South normal fault was noted running parallel with the southern extension of the Malabuyoc anticline. This fault was intersected by Malabuyoc-1 well (CPR, 1976).

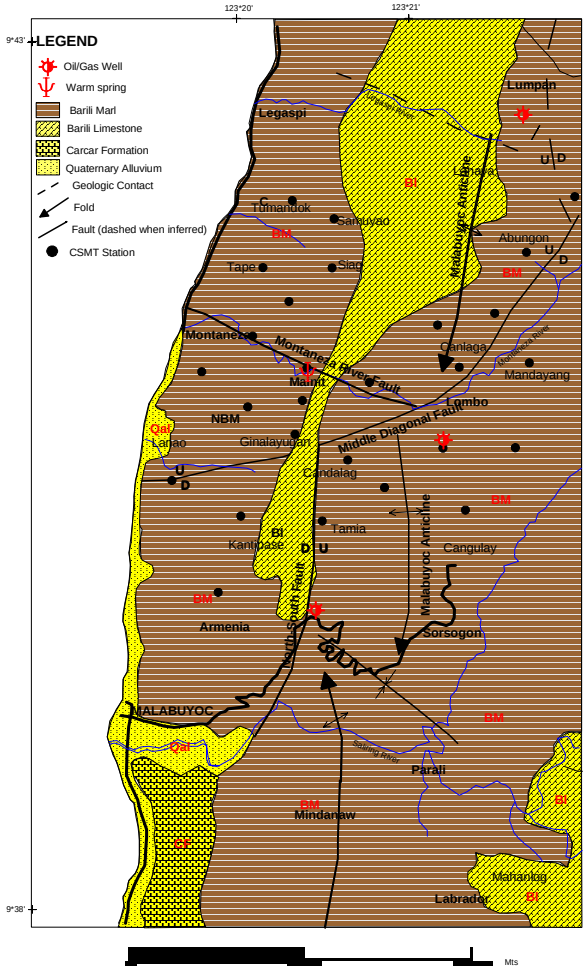

Figure 3: Geology of Malabuyoc Thermal Prospect

The prospect and its surrounding environs are basically underlain by the Mio-Pliocene marine sediments consisting of Barili Formation and Quaternary alluvium (CPR, 1976; MGB, 1985; Malapitan and Del Rosario, 2002) (Fig. 3). Barili Formation is the most dominant rock type in the survey area while the Alluvium consisting of detrital sediments, flood plain debris, coral reefs and gravel deposits abounds the coastlines, riverbanks and lowland areas. Barili Formation is subdivided into Barili marl and Barili

limestone members (MGB, 1985). The Barili marl is poorly bedded, slightly sandy and with occasional thin beds of limestone (MGB, 1985). The Barili limestone is generally dense, massive, white to buff and locally coralline. It occupies the topographic high displaying karst, gorge and knife-edge features.

1.4 Thermal Manifestation

Thermal manifestation occurs as two separate warm spring seepages approximately 20-m apart at Montañeza River in Sitio Mainit, Brgy. Montañeza. The first thermal spring, which is the hotter, discharges from the crevices of the lower limestone member at left bank upstream while the second spring, diluted by the river water comes out from the pile of river deposit at the middle of Montañeza River. The first spring, entombed in a concrete box has a discharge temperature of 56^0 C, neutral pH and flowrate of 2 l/sec while second spring partly amidst river deposits has indeterminate temperature and flowrate due to dilution of river water (BED, 1979; Malapitan and Del Rosario, 2002). Both springs discharge crystal clear and lightly steaming water with faint H_2S odor. No significant hydrothermal alteration was observed at the thermal spring site. Chemistry of the thermal water does not indicate thermal fluid mixing and the associated gas is believed due to decomposition of the organic materials in the marine clastics or from petroleum gas trapped in the reef limestone (BED-ELC, 1979; Malapitan and Del Rosario, 2002). The alignments of the two warm seepage possibly suggest structurally controlled springs.

1.5 Previous Works

The surrounding region of the survey area is well studied for gas and coal occurrences. Early interest in geothermal prospecting was done in 1979 through the initiatives of the Bureau of Energy Development and ElectroConsult (BED-ELC) under the project “Regional Inventory of Philippine Geothermal Areas”. The effort led to the identification of warm spring occurrences in Malabuyoc, Oslob and Catmon. In 1995, Monzon and Pendon of Department of Energy-Energy Resource Development Bureau (DOE-ERDB) reassessed the area for direct and agro-industrial application. In 2001, Malapitan and Del Rosario of DOE-ERDB, conducted geological/hydrological survey of the prospect leading to the identification of the different lithologies and the hydrological mechanics of the geothermal prospect.

2. BASIC PRINCIPLES AND SURVEY METHODOLOGIES

2.1 Basic Principles

The CSMT method uses induced artificial electromagnetic waves to determine the subsurface electrical resistivity structure. These waves originate from a finite source (transmitter dipole), propagate in the earth and “sensed” by another set of instrument known as the receiver. The ratio of the intersection of the “sensed” horizontal electric and magnetic fields yields the subsurface resistivity. The method utilizes an artificial source similar to direct current (DC) method wherein an electrical current is introduce to the ground to produce an electrical signal. The signal travels to the ground in the form of waves of varying frequencies. Low frequency waves penetrate further into the ground than high frequency waves and varying resistivity at depth could be measured from these frequencies.

2.2 Survey Methodologies

A total of 31 CSMT stations were occupied (Fig. 4). Stations were randomly distributed to an average areal distance of 1 kilometer between stations covering the Barangays of Montañeza, Lumbo, Armenia, Tolosa and Sorsogon all in Malabuyoc and Barangays Legaspi, Lumpan and Mompeller in Alegria. Acquisition of resistivity data is through a receiver capable of receiving, collecting and processing telluric and magnetic signals at 14 different frequencies ranging from 5,120 Hz to 0.625 Hz. Measurements of data were carried out in random style utilizing a "fixed" transmitter site and a roving receiver site spaced 3-6 km apart. The transmitter, which is approximately 1.4 km. and oriented N85^{o}E was placed in Sitio Parale, Barangay Mindanao, Malabuyoc which is more or less perpendicular to the general trend of structures in the area. Locations of the proposed station in the field were verified using 1:50,000 M scales map, GPS and thommen altimeter. Since transmitting and receiving was done on the same frequency and simultaneously at a given time, the clock at the transmitter and receiver sites were synchronized first before going out to the field.

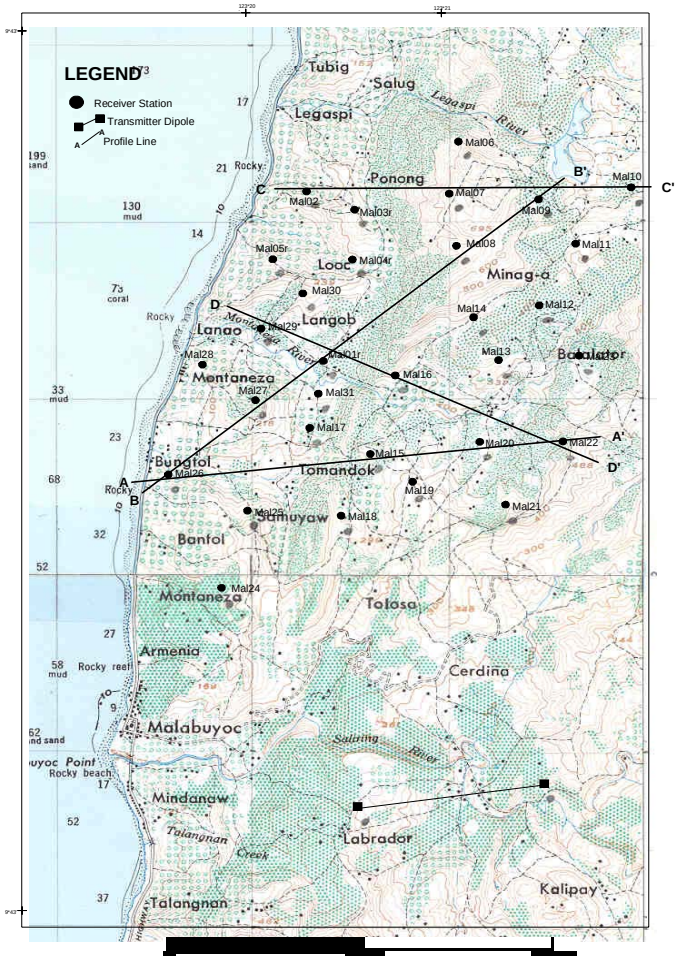

Figure 4: CSMT Station and Location of Profile Lines

3. DATA PROCESSING AND ANALYSIS

The time series data, written in text format are then downloaded and processed using the CSMT 1-D inversion software. A flowchart of CSMT data processing and inversion is shown in Figure 5. Initial processing of the data starts with data sorting rejecting bad or extreme data. The sorted data are then smoothened and interpolated using the spline function. A 1-D inversion is then performed either through resistivity and phase or by phase only. It should be

noted that only the data of the far field are analyzed in the inversion process. Another option is given on the program wherein both Far field data and Near field data are analyze.

In the inversion process, two options were given to the user to produce 1-D plot: 1) the No Input Layer Structure wherein the program automatically assigned the number of layer models/frequency and 2) the Yes Input Layer Structure wherein the user had the hand on the number of layer models. Both options require station elevation and maximum penetration depth in order to calculate the true resistivity, depth and thickness of each layer.

Far field 1D inversion of the data was performed using both the resistivity and phase. Static effects were noted and correlated with the average resistivity curve of the area. We allow the program to automatically assign the number of layers. The maximum depth of penetration used for input for the inversion was 2,000 meters. The depth of investigation is related to the square root of ground resistivity and the inverse square root of signal frequency. CSMT depth of investigation is roughly equal to skin depth (δ) / $\sqrt{}$ 2. Assuming a background resistivity of 100 ohmmeter, sounding to about 2.5 Hz will get an equivalent depth of investigation of about 2,000 meters. Soundings up to 0.625 Hz will give an equivalent depth of investigation much deeper. Studies and practical applications have shown that the maximum usable depth is usually between 2 to 3 kilometers.

The final product is a resistivity-phase-frequency plot of curve trends and distribution of data sets per frequencies. Incorporated in the plots are the average field (measured) and calculated resistivities obtained during the measurement as well as the depth, thickness and true resistivities per layer.

The decision to reject or retest station was based on the results of initial processing. Station with wider range of data set per frequency and no apparent curve trend is subject for retesting.

After initial processing, the data was subjected to further processing to produce a more refine and acceptable data for interpretation. The resistivity and phase plots of the individual station were examined for possible error, noise and surficial effects. To determine the occurrences of near field effect and to visualize clear similarities in trend at depth of the inverted data, correlation among different variables such as apparent resistivity, frequency and depth were made using MSExcel and Grapher programs. After inversion, the data were processed further and was finally linked to Surfer, a mapping software to produce isoresistivity maps and cross sections. The data are interpolated and further smoothened during the process.

Noise analysis, shows that majority of the stations have good readings in almost all frequencies. A few of the stations have scattered data particularly in the lowermost and shallow frequencies. Data for 0.625 Hz are generally noisy and scattered and we have some reservations of the quality of data at this frequency. Each station was analyzed based on the compactness and closeness of the data population in a particular frequency. Good data give us more confidence in the interpretation and have better fit after inversion.

Examination of the resistivity-phase-frequency plots show that the measured and inverted resistivity values of most of the stations depict a similarity of trend. This is shown by increasing resistivities in the uppermost bands, decreasing resistivity in the middle to lower band and increasing again up to the lowermost band.

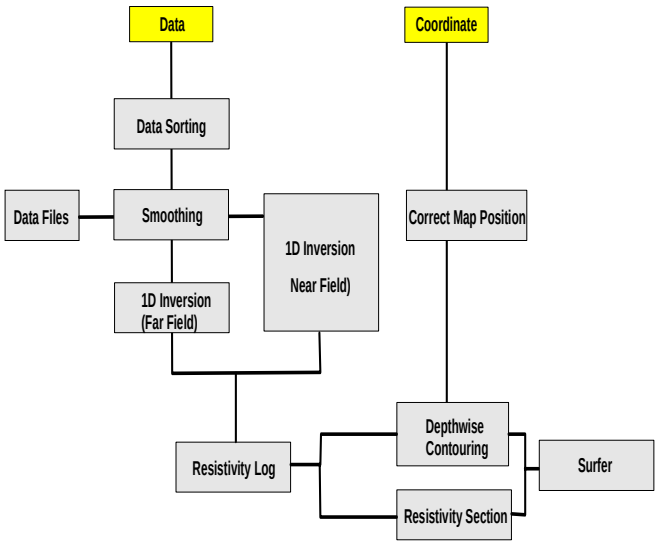

Figure 5: Flow chart of CSMT data processing

3.1 Pertinent Well Information

Three wells seeking natural gas and oil were drilled within the survey area (Fig. 6). Information derived from these wells did not have much bearing with geothermal fluid prospecting except for information related to geology and permeability. Below are brief descriptions of the wells.

3.1.1 CPR-1

The well was drilled at the eastern flank of the Malabuyoc anticline for testing the middle diagonal fault and the possible anticlinal trap at the Malabuyoc anticline. Lithologies were the Upper Miocene to Pliocene marine sediments consisting of Barili Marl, the upper, middle and lower members of the Barili Formation and the clastic member of the Maingit Formation. Lost circulation zones were encountered at depth between –117 to –257-m and –484-m bsl respectively. CPR-1 has a total depth 1,588-m and has a maximum recordable temperature of 54^0C (CPR, 1976).

3.1.2 CPR-2

The well is located about 2.3 km SW of CPR-1 within the western flank of Malabuyoc anticline. It is the second well drilled by Chinese Petroleum Corporation in January 1975 with a purpose of testing the NNE normal fault and the anticlinal traps on the south of the Malabuyoc anticline. Lithologies penetrated by the well were the Lower Miocene to Pliocene marine sediments consisting of the upper and lower limestone member of Barili Formation, the clastic and limestone member of the Maingit Formation, the upper and lower limestone member of Toledo Formatio and the clastic member of the Malubog Formation. Lost circulation zone were encountered at a depth between –17 m and –178 m and between –1085 m and –1093 m bsl respectively. CPR-2 has a total depth of 2,045 m and with maximum recordable temperature of 91^0C (BED-ELC, 1979).

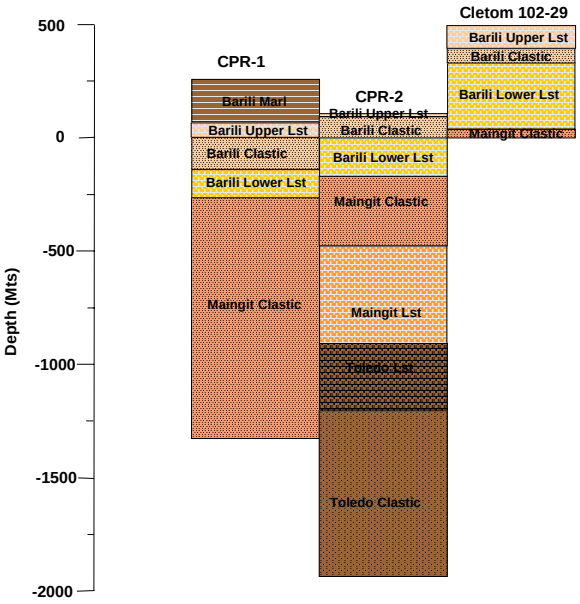

Figure 6: Lithologic Profile of Well CPR-1, CPR-2 and Cletom 102-29

3.1.3 Cletom 102A-29

The well is approximately 3.3 km NNE of CPR-1 within Lumpan, Alegria. There is not much pertinent information from this well except that the penetrated lithologies were similar to that of the CPR-1 and CPR-2 wells. It has a total depth of 716 m.

4. RESULTS OF THE CSMT DATA ANALYSIS

4.1 Isoresistivity Plan Map

Isoresistivity contour maps and resistivity cross sections were prepared to determine the distribution of resistivity at depth. These maps and cross sections are based on the 1-D inversion of CSMT data and are correlated with other relevant information such as geology and structures, well data, etc. This will serve as the basis of interpretation of the geothermal system present in the area.

4.1.1 -50 m bsl

At –50 m bsl, a north-south trending low resistivity anomaly of <10 ohm meter was noted and termed the Ginalayugan-Kantipase anomaly (Fig. 7). This anomaly roughly coincides with the direction of North-South trending fault. Another low resistivity anomaly of <10 ohm meter termed the Lower Lombo anomaly was noted in Lombo which seems to follow the direction of the middle diagonal fault. These suggest structural affinity.

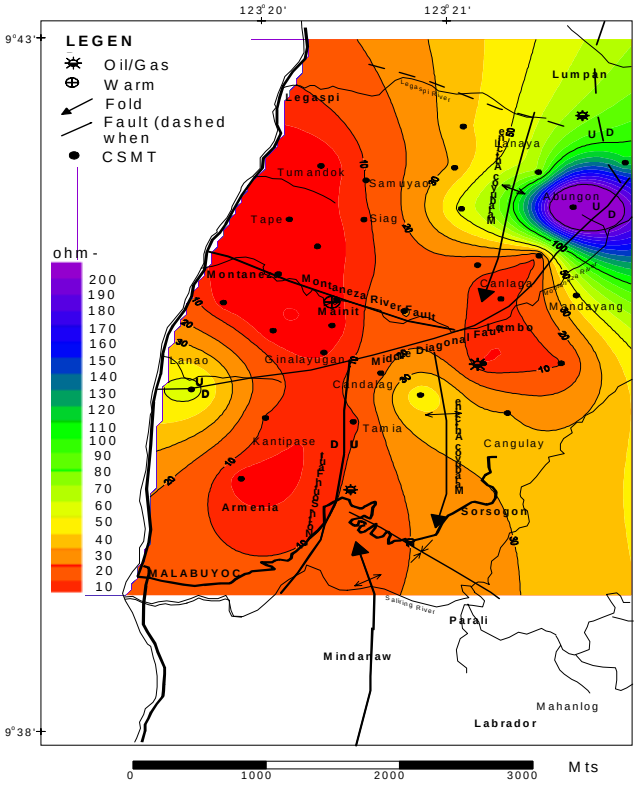

Figure 7: Isoresistivity Contour Map at –50 m below sea level (bsl)

4.1.2 -100 m bsl

At –100 m bsl, the Lower Lombo anomaly decrease in size while the Ginalayugan-Kantipase anomaly increased and practically covers western part of the survey area (Fig. 8). The anomaly widens at the direction of MRF and middle diagonal fault while its southern edge still coincides with trend of North-South trending fault. The widening feature probably suggests the fault as possible conduit for the thermal spring in Montañeza River.

4.1.3 -150 m bsl

The Ginalayugan-Kantipase anomaly decreases in this horizon and is still confined at the western part of the area while the Lower Lombo anomaly breaks down into two segments. Conspicuous here is the intertounging feature of the 20-ohm meter contour beyond the middle diagonal fault. This perhaps suggests either the existence of a possible extension of MRF beyond the middle diagonal fault or some sort of a collapse feature brought about by the movement of middle diagonal fault.

4.1.4 -200 m bsl

The Ginalayugan-Kantipase and lower Lombo anomalies are now joined with each other forming a single anomaly that extends beyond the intersection of the middle diagonal fault and MRF (Fig. 9). This anomaly could indicate the presence of hot fluid at this depth along MRF.

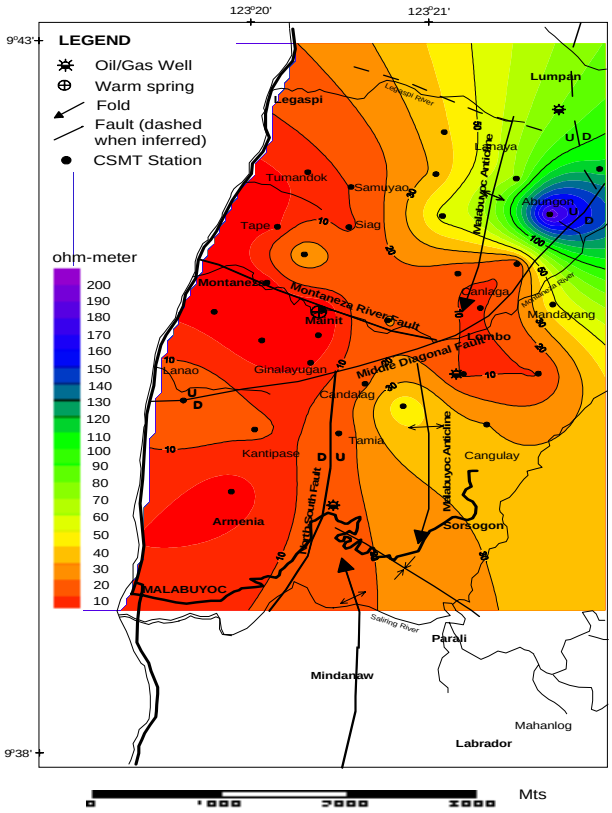

Figure 8: Isoresistivity Contour Map at –100 m below sea level (bsl)

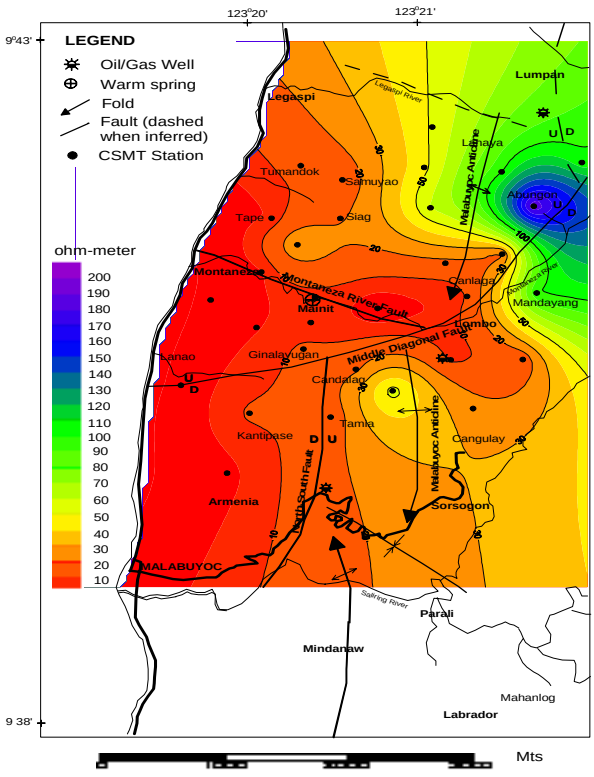

Figure 9: Isoresistivity Contour Map at –200 m below sea level (bsl)

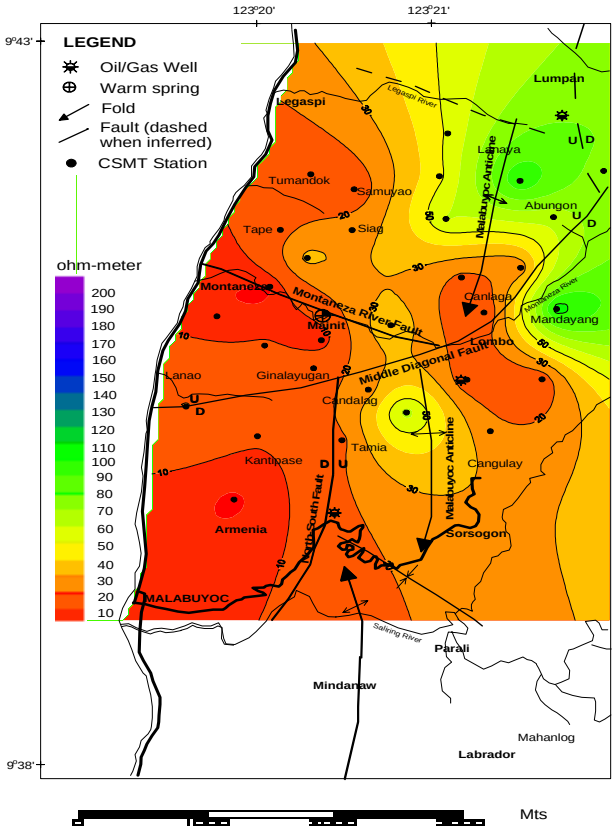

Figure 10: Isoresistivity Contour Map at –300 m below sea level (bsl)

4.1.6 -300 m bsl

The anomaly decreases considerably in size and breaks down into two smaller segments termed here as the Mainit and the Armenia anomalies (Fig. 10). These two anomalies are bounded on the east by highly resistive blocks. The Mainit anomaly trends NW along MRF while the Armenia anomaly lies immediately west of the north trending fault. Conspicuous in this level is the looming of an almost north-south trending middle resistive block that seems to coincide with the trend of the south Malabuyoc anticline.

4.1.7 -400 m and –500 m bsl

The Mainit and Armenia anomalies remain the same. The middle resistive block increases in size.

4.1.8 -750 m

The Mainit anomaly remains the same while the Armenia anomaly increases tremendously in this level (Fig. 11). On the other hand, the middle resistive block increases in size and is merged with the highly resistive block. Conspicuous is the steepening of the contour at the southern edge of the survey area, which probably indicates manifestation of the north-south trending fault. The trend of the resistive block coincides with the trend of Malabuyoc anticline.

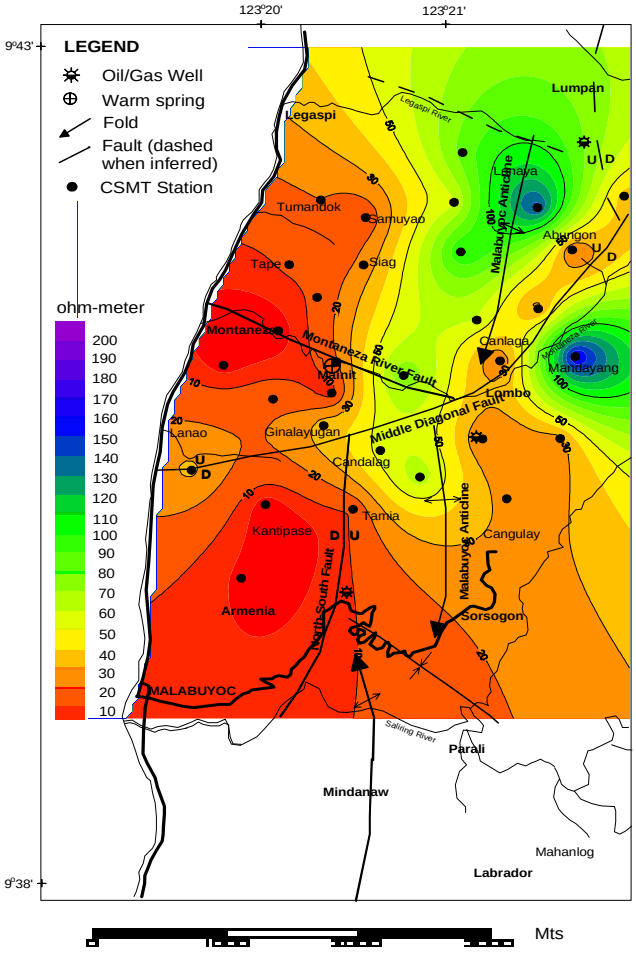

Figure 11: Isoresistivity Contour Map at –750 m below sea level (bsl)

4.2 Isoresistivity Profile

Four isoresistivity profiles were constructed to visualize the subsurface configuration of the survey area. These are Line A-A which transects the central portion of the survey area, Line B-B which trends NE-SW cutting MRF, Line C-C dissecting the northern edge of the survey area and Line D-D paralleling the MRF and cutting the middle diagonal fault (Please refer back to Fig. 4).

4.2.1 Line A-A

The traversed line is generally underlain by high resistive blocks (>50 ohm meter) (Fig. 12). Lying underneath were isolated bodies of middle conductive layer (<20-ohm meter) separated at near surface by middle resistive body (>20 oh meter).

4.2.2 Line B-B

This profile trends NE –SW passing through the thermal spring (Fig. 13). The line is characterized by wide and thick fault-bounded low resistive anomaly at the southwest and high resistive block in the northeast. A 10-ohm meter contour at depth of -200 to -300 m is thought to represent an aquifer that seems to be related to the hot spring. The resistivity contrast indicates the presence of MRF.

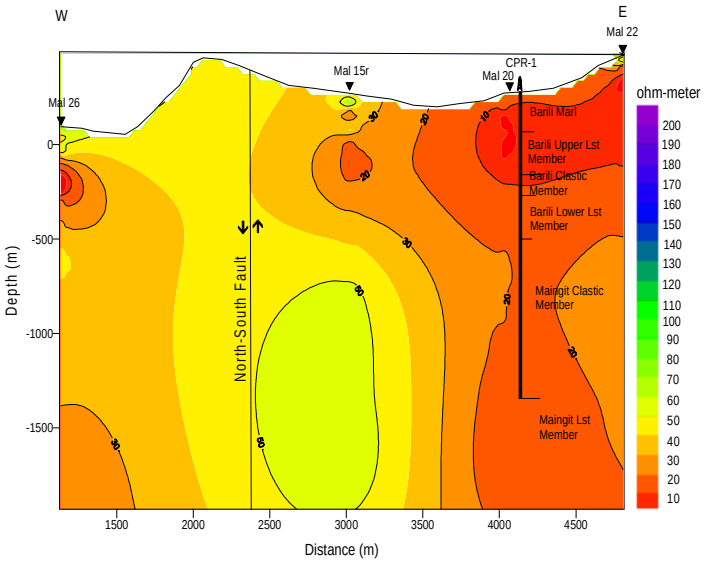

Figure 12: Isoresistivity Profile along Line A-A'

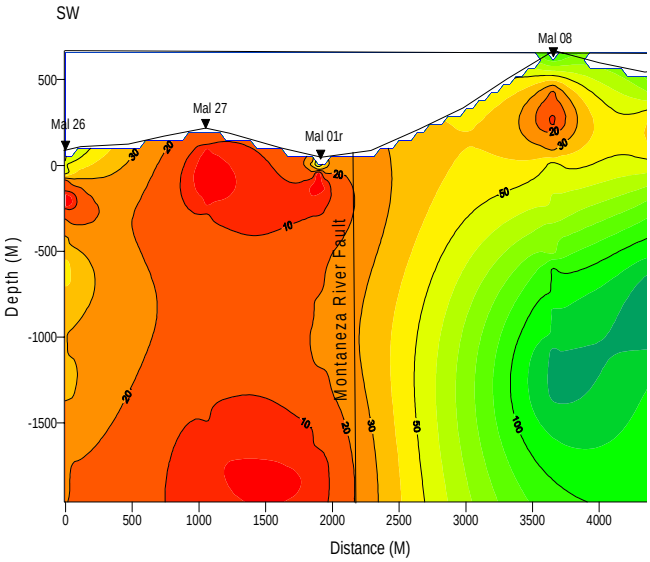

Figure 13: Isoresistivity Profile along Line B-B'

4.2.3 Line C-C

This section transects the northern portion of the survey area (Fig. 14). It also runs perpendicular to the northern segment of the Malabuyoc anticline and the postulated north trending gravity fault in Lumpan area. The line is characterized by a very thick low resistivity anomaly and is bounded on the east by a high resistivity block. The anomaly spreads laterally towards the east capped by high resistive values. Conspicuous also on this section is the down thrusting of the resistivity contour in the east, which could be the manifestation at depth of the postulated fault occurring in the Lumpan area.

4.2.4 Line D-D

This line dissects the middle portion of the survey area (Fig. 15). This section was done to determine the outflow of thermal fluid postulated to be originating east of the survey area. The section is characterized by fault bounded high resistive blocks occurring beneath and a very thick low resistivity anomaly on the NNW existing underneath. Serving as their boundary was the steep resistivity gradient postulated to be the manifestation of North-South Fault and middle diagonal fault at depth. A low resistivity anomaly

noted on the SSE side of the line was gradually increasing at depth and was overlain by high resistive capping. Probable manifestation of the Montañeza river fault at depth was noted through the lateral swaying of the <10-ohmmeter contour at shallow depth and presence of a middle conductive layer in between the resistive block. The middle conductive layer could either be a karsts aquifer or containing part of the heated fluid that is channeled along the MRF.

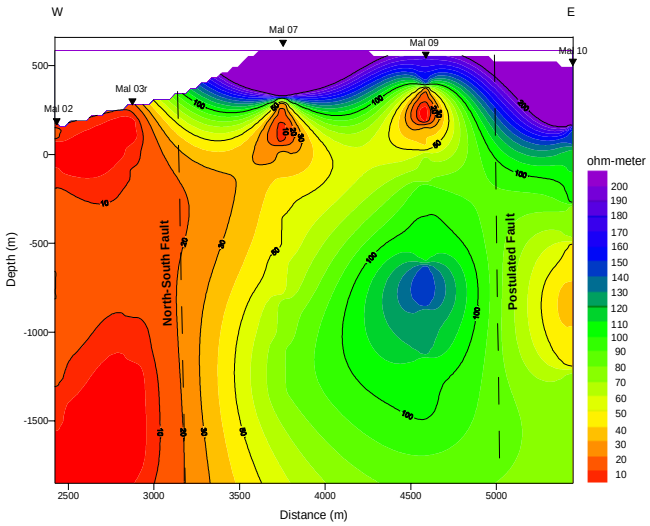

Figure 14: Isoresistivity Profile along Line C-C'

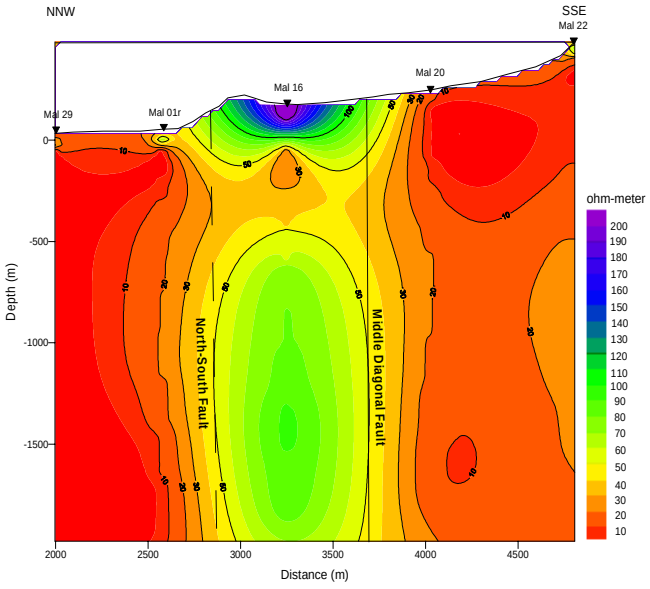

Figure 15: Isoresistivity Profile along Line D-D'

5. DISCUSSION OF THE RESULTS

To understand the geological significance and geothermal implications of the CSMT result, the modeled isoresistivity maps and profiles were correlated with the existing geological and well studies done within the survey area.

Results of correlation show that the resistively structure of the thermal prospect was largely controlled by geological structure. Foremost of these structures were the north-south trending fault that delineates the conductive and resistive zones, the Malabuyoc anticline, MRF and the middle diagonal fault. The result is also synonymous with the postulated anticlinal structure concept of CPRS and geological mapping of Malapitan and Del Rosario (2002). The conductive zone generally lies on the western section of the survey area trending N-S. It is characterized by a coastal wide resistivity low from Sitio Tumandok to the north down to Armenia in the south. It lies within the intersection of middle diagonal fault and MRF and the downthrown side of the north-south trending fault. The downhrown block, being a permeable zone, provides an excellent venue either for hot/cold or seawater accumulation or combination of both. The influence of seawater incursion is evident considering the trend of the resistivity anomaly relative to the sea. Montaneza warm spring seepage is within this zone and along the trace of MRF. The presence of middle diagonal fault is best depicted by the alignment of < 40 ohm meter contour at depth –250 m, -500 m and –750 m bsl respectively while the existence of MRF is exemplified by the deepening and widening of the 10 ohm meter contour at –200 m and –250 m bsl respectively. The faulted anticlinal structure environment, which had been established by previous studies, was proven by this study. This geological concept is manifested by the plunging of the <40-ohm meter contours in the A-A profile. In the isoresistivity map, it is marked by the doming and "ridge effect" of the resistivity contour roughly coinciding with the trend of Malabuyoc anticline.

Though the resistivity results reflect the subsuface structural picture of the survey area, variation in resistivity, however, did not reflect the formational boundary nor the lithological differences of the rock mapped in the survey area owing to the wide range of resistivities in sedimentary rocks. The lithologies penetrated by the three wells were used as determinant factor in the modeling process. Near the wells, the topmost high resistive layer probably correspond to the isolated limestone beds capping the Barili Marl while the middle conductive layer (<10 ohm meter) could either be the Barili Marl or the Barili Upper Limestone member. The presence of clay makes the Barili Marl highly conductive and the low resistivity signature in the limestone could be due to its water-saturated vug and cavities. The middle resistive bodies at depth of –1000 m bsl probably correspond to the clastic and limestone member of the Maingit Formation while at lower depth it might be the lower limestone member of Barili Formation. This assertion is made possible by the fact that the lower limestone member penetrated by CPR-1 is harder, denser and more crystallized than the upper limestone member.

6. GEOPHYSICAL MODEL

Due to absence of mappable igneous rocks that will warrant existence of a possible heat source that will trigger convection, the system in the area was modeled to be similar to a basement aquifer beneath sedimentary basins as shown by their remarkable resemblance.

- A typical basement aquifer occurring beneath sedimentary basin is characterized by the presence of a highly permeable aquifer within or near the top of the basement covered by a sequence of younger sedimentary rocks of low permeability (Hochstein and Yang, 1988). Similarly, serving as the basement for the Malabuyoc system was the resistive lower limestone member of the Barili formation and the clastics and limestone member of the Maingit formation while the aquifer is the karstic low resistive upper limestone

member of the Barili Formation. It is in turn covered by low permeable highly resistive limestone capping the Barili Marl.

- Basement aquifer system occurs beneath the flank of the basin or in anticline and constitutes a low temperature resource and fluids with temperature ranging from 50^0 C to 65^0C. Correlatively, resistivity results depict a faulted anticlinal structure that is consistent with the recently concluded geological mapping conducted by Malapitan and Del Rosario and to the drilling and seismic studies of Chinese Petroleum Corporation. Montañeza warm springs occur at the flank of the postulated Malabuyoc anticline having a discharge temperature of 56^0C. It is a low temperature resource with subsurface temperature ranging from 61-68^0C. Chemistry of the fluid probably derived from marine sediments.

- Basement aquifer system was relatively shallow occurring from 0.5 – 1-km depth. Relatively, the aquifer of the Malabuyoc system was shallow occurring between the 200 – 400 m depth below the surface as shown from the generated isoresistivity map and profiles. Likewise, lost circulation indicating permeable zones was encountered several times between the depth –117 to –257 m bsl from the drill logs of CPR-1 and between the depth –17 to –178 m bsl of the drill log of CPR-2.

Having established the nature and type of the Malabuyoc thermal system, it can be inferred that the aquifer system is situated within the middle diagonal fault and MRF as outlined by 10-ohm meter contour at depth –250 m bsl. The heated fluid probably originates within the center of the basin at the eastern portion of the survey area, was channeled along the middle diagonal fault and MRF and later emerges as warm spring seepage at Montañeza River. The source of an abnormal thermal gradient that trigger forced convection can be postulated as a trapped heat either due to the relatively high thermal conductivity of the basement rock or due to deep burial or extensive sedimentary veneer.

If a well is to be drilled in the area for the purpose of extracting possible hot water for spa and resort development, the best target site is an area bounded by steep resistivity gradient coincident with MRF. The depth of the well should be within the range of –100 m to –300 m bsl to be able to hit the permeable aquifer zone.

7. SUMMARY AND CONCLUSION

Modeling of resistivity results depicts a faulted anticlinal structure. Resistivity anomalies of the prospect were largely controlled by fault structures with the Montañeza warm spring occurring at the western flank of the north trending Malabuyoc anticline. However, resistivity variation did not reflect the formational boundary nor the lithological differences of the various rocks mapped in the survey area. As such the lithologies penetrated by the nearby wells were used in showing the geothermal implication of the resistivity results. Malabuyoc system was categorized as a basement aquifer beneath sedimentary basins with the heated fluid probably originating at the center of the basin located east of the survey area. The fluid was channeled along the middle diagonal and Montañeza river faults and emerged at Montañeza River as warm seepage.

The best target site to drill a well for spa and resort development is the area bounded by steep resistivity gradient coincident with MRF. Possible hot water can be extracted from permeable karst aquifer between depth –100 to –300 m bsl. Correlatively, these are the lost circulation zones encountered from CPR-1 and CPR-2 wells.

Given the above-mentioned results, the just concluded survey in Malabuyoc has delineated possible presence of an aquifer at shallow-medium depths. The real nature of this aquifer has to be established by drilling.

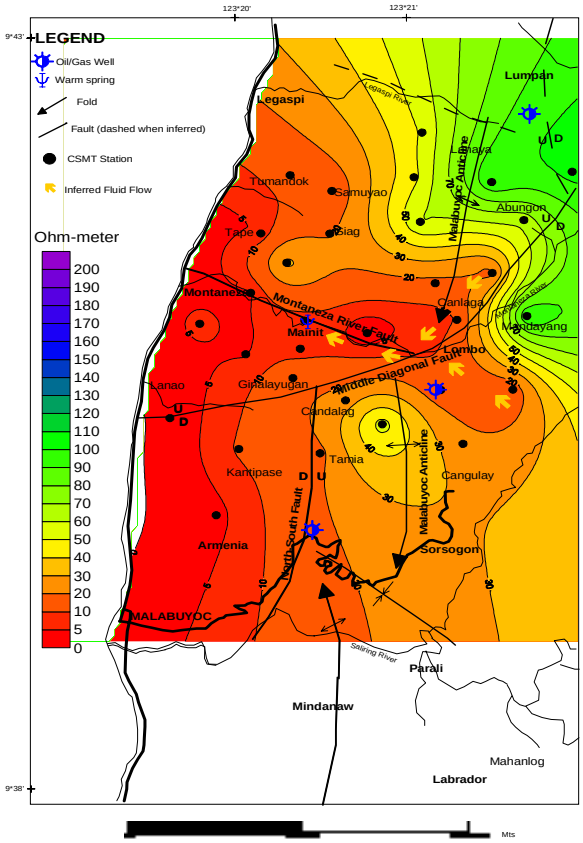

Figure 16: Geophysical Model of Malabuyoc Thermal System (at –250 m below sea level)

8. ACKNOWLEDGMENT

The authors would like to thank the following persons who contributed to the success of the survey:

Mr. Vicente M. Karunungan, our Division Chief; Director Antonio Labios, Gerald Cabizares, Richard Russel and Enric Padayao of DOE-Visayas Field Office; Mayor Lito Creus of the Malabuyoc town for logistic support; Ms. Alicia Reyes for her geophysical comment and edition of this report; and to the Department of Tourism and Department of Health for their continued trust and believe to ERDB-DOE technical.

REFERENCES

Bureau of Energy Development. 1979. :Inventory of the Thermal Areas in the Philippines, Philippine-Italian Technical Cooperation on Geothermics Stage II, DOE Internal Report, Pp 2

Del Rosario, R.A., Pastor, M.S., Malapitan, R.T., Papasin, R.F. and Domingo, F.G. 2002.:Comparative Study of the 1999 and 2001 Controlled Source Magnetotelluric Surveys Done in Manito Lowland Geothermal Resource, Manito, Albay, DOE Internal Report, 61pp.

Del Rosario, R.A., Papasin, R.F. and Domingo, F.G. 2000.: Controlled Source Magnetotelluric Survey of Mabini Geothermal Prospect, Mabini, Batangas. DOE Internal Report.

Hersir, Gylfi Pall and Bjornsson, Axel. 1991.: Geophysical Exploration for Geothermal Resources Principles and Application, UNU Geothermal Training Program Report 15, 88 pp.

Hochstein, M. P. 1990.: Classification and Assessment of Geothermal Resources. UNITAR/UNDP, p 31-57

Hsieh, S. H. and Hsu, C. H. 1974.: Well Completion Report of the CPR-1 Well Alegria-Malabuyoc Anticline, Cebu, Philippines, Chinese Petroleum Corporation, 39 pp

Hsieh, S. H. and Hsu, C. H. 1975.: Well Completion Report of the CPR-2 Well Alegria-Malabuyoc Anticline, Cebu, Philippines, Chinese Petroleum Corporation, 50 p.

Hsieh, S. H. and Hsu, L. M. 1977.: Well Completion Report of the Malabuyoc- Well Alegria-Malabuyoc Anticline, Cebu, Philippines, Chinese Petroleum Corporation, 25 pp

Malapitan, R.T. and Del Rosario, R. A. 2002.: Geology and Hydrology of Malabuyoc Geothermal Prospect, Malabuyoc, Cebu, DOE Internal Report.

Mines and Geosciences Bureau. 1982.: Stratigraphy of Southern Cebu. Geology and Mineral Resources of the Philippines Vol.1

Pendon, R.R. and Monzon, B. J. 1996.: Cebu Geothermal Prospects, DOE Internal Report

Philippine Bureau of Mines. 1956.: Geology and Coal Resosurces of the Argao-Dalaguete Region, Cebu, Special Project Series. Publication No. 7, 50 pp

Robertson Research International Ltd. 1977.: The Philippines: An Evaluation of Coal Resources, Atlas. Vol 2

Santos-Ynigo,L. 1951.: Geology and Ore Deposits of Central Cebu, Bureau of Mines Internal Report

Wardell, A. 1985.: Report on Coal Resources of the Philippines, RP-UK Coal Resource Study

Zonge, K. L. and Hughes, L. J. 1992.: Controlled Source Audio-Frequency Magnetotellurics, Society of Exploration Geophysicists, Investigation in Geophysics No.13, p 713-807.

Zonge, K. L. 1992.: Introduction to CSAMT, Northwest Mining Association, Practical Geophysics II for the Exploration Geologists, p 440-49